

The Cr redox record of fO_2 variation in angrites. Evidence for redox conditions of angrite petrogenesis and parent body. Charles, K. Shearer¹, Aaron S. Bell¹, Paul V. Burger¹, James J. Papike¹, John Jones², and Loan Le².

¹Institute of Meteoritics, Department of Earth and Planetary Science, University of New Mexico, Albuquerque, New Mexico 87131, ²NASA Johnson Space Center, Houston, TX 77058.

Introduction: Angrites represent some of the earliest stages of planetesimal differentiation [e.g. 1-5]. Not surprisingly, there is no simple petrogenetic model for their origin [1-10]. Petrogenesis has been linked to both magmatic and impact processes [1-10]. Studies by [6,7] demonstrated that melting of chondritic material (e.g. CM, CV) at redox conditions where pure iron metal is unstable (e.g., IW+1 to IW+2) produced angrite-like melts. Alternatively, [8-9] suggested that angrites were produced at more reducing conditions (<IW) with their exotic melt compositions resulting from carbonates in the source or from nebular condensation. Clearly, understanding what role fO_2 plays in producing angrite magmas is critical for deciphering their petrogenesis and extending our understanding of primordial melting of asteroids. Calculations for the fO_2 conditions of angrite crystallization are limited, and only preliminary attempts been made to understand the changes in fO_2 that occurred during petrogenesis. Many of the angrites have phase assemblages which provide conflicting signals about redox conditions during crystallization (e.g., Fe metal and a Fe-Ti oxide with potential Fe^{3+} , i.e., [5,11-12]. There have been several estimates of fO_2 for angrites [5,11-15]. Most notably, experiments by [11] examined the variation of D_{En}/D_{Gd} with fO_2 , between plagioclase and fassaite pyroxene in equilibrium with an angrite melt composition. They used their observations to estimate the fO_2 of crystallization to be approximately IW+0.6 for angrite LEW 86010. This estimate is only a “snapshot” of fO_2 conditions during co-crystallization of plagioclase and pyroxene. Preliminary XANES analyses of V redox state in pyroxenes from D’Orbigny reported changes in fO_2 from IW-0.7 during early pyroxene crystallization to IW+0.5 during later episodes of pyroxene crystallization [15]. As this was a preliminary report, it presented limited information concerning the effects of pyroxene orientation and composition on the V valence measurements, and the effect of melt composition on valence and partitioning behavior of V. A closer examination of fO_2 as recorded by Cr valence state in olivine will allow us to test models for primordial melting of chondritic material to produce the angrite parent melts. Here, we report the our initial stages of examining the origin and conditions of primordial melting on the angrite parent body and test some of the above models by integrating an experimental study of Cr and V valence partitioning between olivine [OL] and an

angrite melt, with micro-scale determinations of Cr and V oxidation state in OL in selected “volcanic” angrites.

Analytical Approach: Thin sections of LEW 87051 and Sahara 99555 were initially examined and documented using backscattered electron imaging (BSE) on the JEOL JXA-8200 Superprobe electron microprobe (EMP) in the Institute of Meteoritics. Wave-length dispersive X-ray maps were collected for Cr, Ca, Mn, P and Ti, while energy dispersive (EDS) maps were collected for Mg and Fe. These maps were collected using a 15 kV accelerating voltage, a 500 nA beam current and a dwell time of 800 ms/pixel. Quantitative point analyses were conducted of various silicates and oxide phases using the EMP. These analyses employed an accelerating voltage of 15 kV, a beam current of 20 nA, and a spot size from 1-3 μ m. Chromium K-edge XANES data were acquired with the X-ray microprobe of GSECARS beamline 13-ID-E at the Advanced Photon Source (APS), Argonne National Laboratory, Illinois. The X-ray source at the APS beamline was a 72-pole, 33 mm period undulator. The beam was focused to a final spot size of 5 μ m by 5 μ m with dynamically configured Kirkpatrick-Baez focusing mirrors. All spectra were acquired in fluorescence mode. The chromium K-edge XANES data are being interpreted for the effects of orientation, melt composition, and temperature as documented by [16-18]. Melting and crystallization experiments are being conducted on Sahara melt compositions to aid in the interpretation of the impact of these variables on Cr and V valence behavior.

Results: A BSE image and selected X-ray maps of OL from LEW 87051 illustrate irregular shaped cores relatively high in Mg# and Cr and low in Ca relative to surrounding olivine (Fig. 1). The OL surrounding these cores exhibit an increase in Fe, Cr and Ca from the irregular core interface to rim. It has been suggested [1,7] that these irregular shaped OL cores are xenocrysts. Chemical variations in the olivine along traverse A-B are illustrated in Figure 2. The location of XANES data point on traverse A-B are shown in the BSE image in Figure 1. The calculated $Cr^{2+}/\Sigma Cr$ ranges from 0.34 to 0.23 in the OL rim to 0.48 to 0.50 in the OL core. This XANES data is plotted within the context of other chemical data in Figure 2. Clearly, this data illustrates that the xenocrystic cores of the OL have a much higher $Cr^{2+}/\Sigma Cr$ than the surrounding OL.

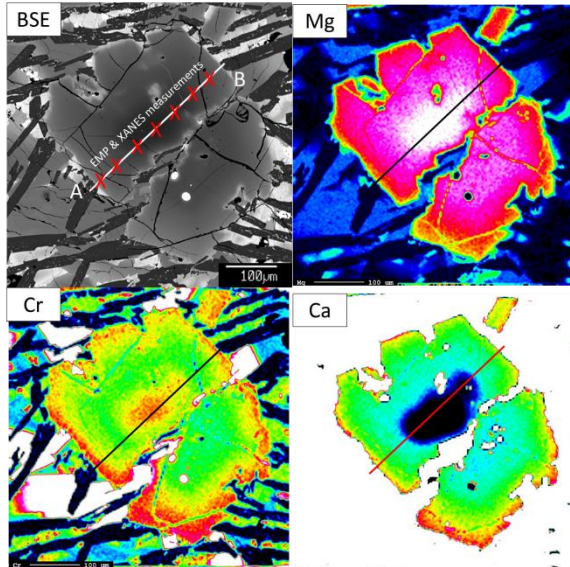


Fig. 1. BSE and X-ray maps of OL in angrite LEW 87051. EMP traverse (A-B) and XANES data points collected along that traverse (X) are illustrated. Data presented in Fig. 2.

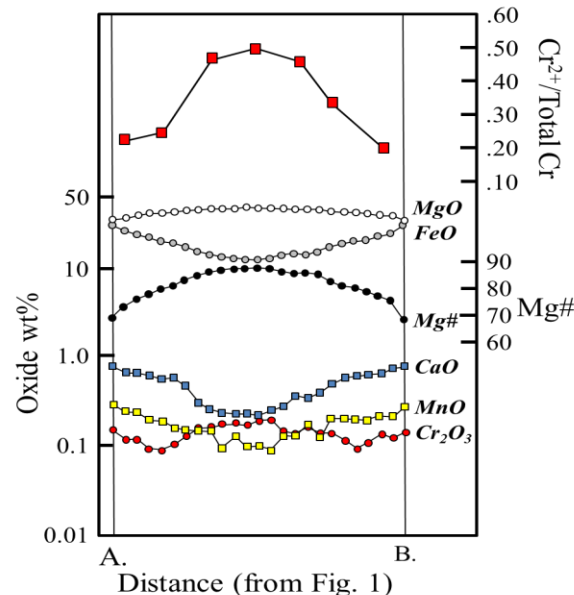


Fig. 2. Variation in MgO, FeO, MnO, CaO, Cr₂O₃, Mg#, and Cr²⁺/ΣCr in an OL traverse illustrated in Fig. 1

Discussion: The relationship between the measured Cr²⁺/ΣCr in OL and fO_2 conditions of the melt system is dependent upon variables such as the orientation of olivine, temperature and melt composition [16-18]. Bell et al. [16-18] illustrated the relationship among all of these variables for a primitive martian basalt composition. This approach enabled a quantitative determination of fO_2 for martian basalts. Reconstructing the fO_2 history from the olivine may be determined based on the observations that (i) the outer olivine rims crystallized at approximately 1170°C [11,19,20], (ii) the b axis is approximately

normal to the plane of the OL in Fig. 1, and (iii) the behavior of Cr²⁺/ΣCr for the OL and angrite melt can be modeled and approximated from our martian basalt data [16,17,21]. From these observations, we calculate that the fO_2 during the crystallization of the outer OL rim was approximately IW+1.8 to IW+2. These preliminary observations and calculations are consistent with the LEW 87051 melt being produced by melting of chondritic material at relatively oxidizing conditions. The higher Cr²⁺/ΣCr and lower Ca observed in the OL core clearly indicates that it is xenocrystic in origin with a distinct redox signature. There are three potential petrogenetic scenarios for the xenocrystic cores: OL originated from a cumulate lithology derived from a much more primitive angrite magma (e.g., dunitic angrite NWA 8535), a remnant from the angrite parent body mantle [10], or a crustal remnant incorporated into an impact melt (e.g. NWA 8535). We can initially examine the origin of the changing redox state of the olivine core by examining two end-member models: (1) variation in Cr due only to changing fO_2 and (2) variation in Cr valence caused only by changing temperature. Assuming that the core crystallized at the same temperature as the rim (1170°C), the calculated fO_2 of core crystallization would be two orders of magnitude more reducing than the rims (IW). On the other hand, if the fO_2 was constant (value of IW+2), the calculated temperature of crystallization would be >1600°C. The latter appears unlikely and we conclude that the redox core signature reflects both a more reducing (~IW) and higher temperature environment (T=1350°C). Ongoing experiments to better understand the behavior of Cr in angrite melts and constrain temperatures of crystallization will be used to assess if these initial observations and conclusions are correct.

References: [1] Mittlefehldt et al. (1998) Chapter 4 In J.J. Papike, Ed., Planetary Materials, 36, p. 1-195. RIM, MSA, Chantilly, VA. [2] Baker et al. (2005) Nature 436, 1127-1131. [3] Amelin (2008) GCA 72, 221-232. [4] Brennecka and Wadhwa (2012) PNAS 109, 9299-9303. [5] Keil (2012) Chemie der Erde 72, 191-218. [6] Jurewicz et al. (1995) GCA 59, 391-408. [7] Mittlefehldt et al. (2002) MAPS 37, 345-369. [8] Kurat et al. (2004). GCA 68, 901-924. [9] Jambon et al. (2005) MAPS 40, 361-375. [10] Mikouchi et al. (2015) 46th LPSC Abstract #2065. [11] McKay (1989) In: RIM 21 (eds. Lipin and McKay) 45-77. [12] Mikouchi et al. (2011) Workshop on the Formation of the First Solids in the Solar System, Kauai. [13] Mikouchi et al. (2008) MAPS 43, A98. [14] Brett et al. (1977) EPSL 35, 363-368. [15] King et al. (2012) 43rd LPSC Abstract #2436. [16] Bell et al. (2014) Am. Min. 99, 1404-1412. [17] Bell et al. (2015) 46th LPSC (this meeting). [18] Bell et al. (2015). [19] Longhi (1999) GCA 63, 573-585. [20] McKibbin and O'Neill (2016) MAPS, in press. [21] Hanson and Jones (1998) Am. Mineral. 83, 669-684.